NASA Contractor Report 172564

SOUND PROPAGATION STUDIES FOR A LARGE

HORIZONTAL AXIS WIND TURBINE

Kevin P. Shepherd

THE BIONETICS CORPORATION
Hampton, Virginia

and

Harvey H. Hubbard

THE COLLEGE OF WILLIAM AND MARY
Williamsburg, Virginia

NASA

National Aeronautics and
Space Administration

Langley Research Center
Hampton, Virginia 23665

OUTLINE

INTRODUCTION

Methods are being developed for predicting the noise from large wind turbine generators. One of the least understood factors is that of sound propagation in windy conditions such as those that are inherent in the normal operations of wind turbines. Although much is known about sound propagation in the atmosphere (see for instance Refs. 1-4) very few measurements have been reported for conditions of high mean wind velocities.

Included in this paper are the results of systemmatic noise measurements in three directions, over a range of distances to 1050 m, over a range of frequencies from 8 Hz to 2000 Hz, and for a stable wind turbine noise source in windy conditions. Refraction due to a mean wind gradient is shown to have sizeable effects on the noise levels at given distances depending on the wind direction.

This effort is part of the Department of Energy wind energy program which is managed by the NASA Lewis Research Center. The WTS-4 (Refs. 5-7) machine was manufactured by the Hamilton Standard Division of United Technologies and is currently operated by the Department of the Interior, Bureau of Land Management.

APPARATUS AND METHODS

Description of Site

Measurements were made at the operational site of the WTS-4 machine near Medicine Bow, Wyoming (Figure 1). The site is located in gently rolling open range territory that has an elevation of about 2075 m (6800 ft.) above sea level and is remote from airports and main highways. There are no trees and only sparse surface vegetation.

-1-

Wind velocity and direction were monitored and recorded continuously from meteorological instruments located at an elevation of 61 m above ground level and at a distance of about 300 m west (upwind) of the machine. For data reported herein the wind direction varied from 270° to 315°, the wind velocity ranged from 9.4 to 13.0 m/s (21 to 29 mph), the relative humidity was 55%, the barometric pressure varied from 788 mB to 791 mB, and the ambient temperature varied from 13° to 17°C. All data were recorded on September 11-13, 1984 and between 800 and 1800 hours.

Description of Wind Turbine Generator

The WTS-4 wind turbine generator has a two bladed, 79.2 m (256.6 ft.) diameter, rotor mounted on an 80 m (263 ft.) high tower with a twelve sided cross section. The distance across the tower, between flats, is 3.66 m (12 ft.). It is a downwind machine (inflow encounters the tower before encountering the rotor) having a rated power output of 4.2 MW. Its operational range of wind velocities is about 7.1 m/s to 27 m/s (15.9 to 60.4 mph). The blades are pitch controlled at the root by a hydraulic control system and rotational speed is maintained at 30 rpm. Blades are tapered in chord from 1.04 m (3.4 ft.) at the tip section (NACA 23012 airfoil) to 4.69 m (15.4 ft.) at the root section (NACA 23036 airfoil). The twist angle varies from approximately -1° at the tip to 16° near the root. Figure 1 shows an insert photograph of the machine in the feathered condition.

Acoustic Measurements

All noise measurements were made with commercially available battery powered instrumentation. One half inch diameter condenser microphones with a useable frequency range 3-20,000 Hz were used with a two channel direct recording tape recorder which provides a dynamic range of about 60 dB and has a

-2-

flat response within ±2 dB in the frequency range of 25 Hz to 20,000 Hz. One microphone channel was unweighted and the other was C-weighted in an attempt to more effectively utilize the available recorder dynamic range.

Data were obtained for distances up to about 1100 m and at azimuth angles of 0° (on-axis upwind), 180° (on-axis downwind), and 270° (in-plane left, facing into the wind). Two identical recording sys ems were used for each measurement condition. One was fixed at a reference location 150 m from the machine in the appropriate direction (0°, 180° or 270°) and the other was moved to the required field measurement location. The resulting pairs of simultaneous measurements made it possible to account for any differences due to changes in the noise output of the wind turbine. Measurement locations are shown in Figure 2 along with their respective elevations above sea level. The terrain is generally flat and line of sight conditions exist between the source and the measurement points. Spectral data were obtained with the aid of conventional one-third octave band and narrow band analyzers. Statistical analyses were performed using a community noise analyzer.

To minimize the detrimental effects of wind noise, polyurethane foam microphone wind screens were used and microphones were placed at the ground surface, where wind velocities were relatively low.

Wind Conditions

Example time histories of wind speed and direction are shown in Figure 3 to illustrate the normal variability observed at the test site. These records indicate that wind speed varies by about ±3 m/s and wind direction varies by about ±6 Deg. The above characterize the behavior of the wind at this site for a number of recordings covering an extended period of time and are thus considered representative of the conditions existing during the present tests.

RESULTS AND DISCUSSION

The results are presented in the form of calculated acoustic ray path diagrams, pressure time histories, narrow band frequency spectra, one-third octave band frequency spectra, amplitude distributions, and overall sound pressure levels. All sound pressure levels are referenced to 20 µpa. Data are arranged to illustrate the effects of distance in three directions relative to the wind vector.

Calculated Acoustic Ray Path Diagrams

A mean wind velocity gradient interacts with an acoustic wave causing it to refract downwards or upwards, depending on whether the wind velocity is in the same or opposite direction to the wave propagation. In order to illustrate this a series of ray path calculations has been made for ranges of source height and wind velocity.

Point Sources. Example results are noted for combinations of source height, wind velocity and distance of interest for large wind turbine applications in the ray diagrams of Figure 4. For these calculations a logarithmic wind gradient (see Appendix) is assumed with a wind velocity at the point source height of 10 m/s and a ground roughness length of 0.1 m. Source heights of 40 m and 120 m are assumed for Figure 4(a) and (b) respectively. Selected rays are shown for both the upwind and downwind directions. The ray patterns are noted to be very similar for the two source heights except that, for a given initial ray angle, the reflections from the ground occur at shorter distances for the lower source height. The patterns are seen to be different in character however depending on whether the direction of propagation is with or against the wind.

-4-

In the downwind direction the rays are bent toward the ground, are reflected upwards, and then bend back toward the ground again. Thus, for a receiver at ground level and at a relatively large distance downwind, destructive or constructive interference may occur when more than one ray (either direct or reflected) intersects the receiver location. For the example presented in Figure 4(a) the shortest distance at which interference occurs for a ground level receiver is approximately 2500 m. Beyond this distance the prediction of sound pressure level becomes difficult. At shorter distances only one ray can intersect any given ground level receiver location. Thus, sound pressure level is predicted to decay with distance according to spherical spreading and atmospheric absorption out to a relatively large distance.

In the upwind direction the rays bend away from the ground. The ray which just grazes the ground defines the start of the shadow zone, into which no direct sound can penetrate, thus resulting in excess attenuation. This shadow is not sharply defined as in the case of an optical shadow and in reality sound energy is diffracted into this shadow region. Also, due to inhomogeneities in the atmosphere, sound energy is scattered into the shadow zone. Thus sound pressure level is predicted to decay with distance according to spherical spreading and atmospheric absorption until the shadow boundary is reached. Beyond this distance, frequency dependent excess attenuation takes place, the lowest frequencies being attenuated the least.

Distributed Sources. The ray path diagram is modified for the case of a distributed source, such as a rotor disk, as indicated in Figure 5. For this illustration the bottom of the disk source is assumed to be at a height of 40 m and the top to be at a height of 120 m and the wind speed is assumed to be 10 m/s at the hub. At any location in the downwind direction sound will be received from every point on the rotor disk. Furthermore, at relatively large

distances (greater than about 2500 m for this example) sound originating from a point on the rotor disk can reach a particular ground level receiver location by at least two different ray paths, the first being a direct ray from source to receiver, the other being a ray which has undergone one or more reflections from the ground surface. Thus at these relatively large distances constructive and destructive interference effects may occur.

In the upwind direction, shadow zone formation will occur for the lower portion of the disk at shorter distances than for the upper portion. The distance to the shadow zone as defined in Figure 5 is determined by the upper portion of the disk and for the assumptions of Figure 4 occurs at a distance of about 600 m. This distance is a function of the wind gradient and the source height and is independent of frequency. As noted previously, the excess attenuation which occurs beyond this distance is frequency dependent.

Source Characteristics

Figure 6 presents a third octave band noise spectrum (64 second averaging time) measured at a distance of 150 m from the base of the machine. At this distance there are essentially no differences between the noise spectra in the upwind and downwind directions. Thus the data of Figure 6 characterize the on-axis noise of the machine. The spectrum peaks at the low frequencies and decays in level as frequency increases. The top inset is a time history of the band level of the one-third octave band having a center frequency of 63 Hz. The averaging time for this trace is 0.2 secs. Maximum values are seen to occur at a period corresponding to the blade passage frequency (1.0 Hz). From observations made at a position close to the machine it was concluded that these maximum sound pressure level values occur when the rotor blades are in the vertical position. This low frequency (thumping) noise, consisting of loading harmonics, is due to the rotor passing through the tower wake in the

-6-

lower portion of the disk. Also shown in Figure 6 is a time history of the band level for the one-third octave band having a center frequency of 1000 Hz. Similar peaks are noted to occur at the blade passage frequency and were also found to correspond to the vertical rotor blade position. In this case though the noise is boundary layer and/or blade trailing edge related. The peak levels are believed to be associated with the top portion of the disk due to higher relative blade speeds and angles of attack resulting from the higher wind speeds.

Effects of Distance

Band Levels. From measured one-third octave band spectra at various distances from the machine the effects of distance on the band levels can be illustrated as in Figures 7, 8 and 9. The levels were derived using a 64 second averaging time.

The data of Figure 7 show the effects of distance in the downwind direction for one-third octave bands having center frequencies f_c of 63, 125, 250, 500 and 1000 Hz. Shown for reference in each case is a curve representing combined effects of atmospheric absorption for the particular frequency (Ref. 1) and spherical spreading. Note that for the range of distances involved, up to about 1000 m, the data fall close to the curves and there is no evidence of excess attenuation due to ground effects nor of destructive or constructive interference due to the effects of refraction and reflection. This latter finding is consistent with the calculations of Figures 4 and 5. Similar data are presented in Figure 8 for the crosswind direction and the conclusions are the same. It should also be noted that the multiple data points at 150 m cluster closely, thus indicating very little variation in the average noise output of the wind turbine during the test.

The decay of sound pressure level with distance in the upwind direction, however, is different as illustrated by the comparison data of Figure 9. The levels in the 630 Hz band are plotted as a function of distance for three different directions. The data for the downwind and crosswind directions follow the computed spherical spreading and atmospheric absorption curves closely but the upwind data fall below the curve beginning at about a distance of 400 m. This result is in qualitative agreement with those of Figures 4 and 5, and indicates the existence of an upwind shadow zone.

The 630 Hz band measurements are replotted in Figure 10(a) along with some computed shadow zone noise levels assuming acoustic point sources at the bottom of the disk, the hub, and the top of the disk respectively. The data seem to fall generally between the curves for the hub and the top of the disk. In Figure 10(b) the computations were repeated assuming a distributed source with the source strength varying according to the fifth power of section speed (see Appendix). In this latter case the data points are in very good agreement except at the extreme distance of 1050 m. This discrepancy may be due either to poor signal to noise ratio for the measurements or to the effects of atmospheric scattering or both.

Distributed source computations were made for the upwind direction for a range of frequencies for comparison with measured data. These comparisons are given in Figure 11 along with the respective spherical spreading and atmospheric absorption curves for reference. There is evidence of shadow zone formations at all of the frequencies and the data points tend to follow the distributed source attenuation curves (dashed lines) except at the extreme distances. It is concluded that estimates of sound pressure level in the upwind direction must account for excess attenuation inside the shadow zone.

Statistical Measures. In order to further explore the distributed source concept and its implications for predicting noise levels as a function of distance the opportunity was taken to evaluate a number of statistical measures as defined in Figure 12. The sound pressure level time history is for the one-third octave band having a center frequency of 630 Hz. The band level averaged over 0.2 secs is shown for about a 30 sec period. The various statistical measures L_1, L_{10}, L_{50}, L_{90} and L_{99} are listed on the right hand side of the figure and their measured values are indicated for the noise sample illustrated. For instance, the sound pressure level value of 60 dB for L_1 means that the instantaneous level of the noise signal was above 60 dB for 1% of the analysis time. Likewise, the L_{99} level of 56 dB indicates that the level of the noise signal was above 56 dB for 99% of the analysis time. Other statistical measures are similarly defined.

Figures 13 and 14 show the levels for various statistical measures as a function of distance for one-third octave band center frequencies of 63 Hz and 630 Hz respectively in the downwind direction. In each case the decay of sound pressure level as a function of distance is noted to be in close agreement with the respective spherical spreading and atmospheric absorption curves of Figures 13 and 14.

The decay rates with distance are the same for all statistical measures. This suggests that the variability in the signals is essentially the same at all measurement distances. This is a surprising result because it indicates that the variability of the signals is not controlled by atmospheric propagation but by the source itself. Furthermore these results indicate that in addition to the average noise output of the source being nearly constant (Figures 7 and 8), the statistical properties of the radiated noise are stable as well.

A different picture emerges from an analysis of statistical measures data for the upwind direction, as shown in Figures 15 and 16. The measured data are seen to fall generally below the reference (solid) curves for spherical spreading and atmospheric absorption, thus confirming the existence of upwind shadow zones. The excess attenuation is greatest at the higher frequency (630 Hz) as was noted in Figure 11. Note that the distance at which the data begin to diverge from the solid curve is different for each statistical measure. This would be expected due to the effects of refraction which cause an acoustic shadow to form from the bottom of the disk at relatively short distances and which affects a larger portion of the disk at greater distances. At distances of 200 – 400 m, the bottom of the disk is apparently shadowed and the entire disk is enveloped at about 600 m. Prediction curves based on the distributed source concepts described in the appendix are shown as dashed lines in Figures 15 and 16. The data points generally follow the dashed curves except at extreme distances. These results, both measured and predicted, clearly show that each of the statistical measures defined in Figure 12 vary differently with distance in the upwind direction.

Thus at relatively short distances at which an acoustic shadow is formed from the bottom of the disk, peak measures such as L_1 and L_{10} are unaffected by the shadow since for some part of each revolution of the wind turbine, both rotor blades are above the "shadowed" part of the disk. Measures such as L_{99} and L_{90} however are affected since for part of each revolution one blade tip is "shadowed." At greater distances, such that more than one half of the disk is shadowed, the peak levels are also affected since one of the blades is always shadowed. This phenomenon is discussed further in the Appendix.

Very Low Frequencies. Narrow band analyses were performed to evaluate the effects of distance on the very low frequency components of the loading harmonics. Because of signal to noise ratio and recorder response considera-

tions, only the components in the range 8 to 16 Hz are included. These components may not be audible but can be significant for noise induced building vibrations. A minimum signal to noise ratio of 3 dB was realized for all of the data included in Figure 17 for both the upwind and downwind directions. The available data for the upwind direction are plotted, with reference to the simultaneously measured data at the 150 m point, in Figure 17(a) along with a spherical spreading curve for reference. The data generally follow the spherical spreading curve, thus suggesting that for the range of distances examined there is effectively no excess attenuation in the upwind shadow zone for these very low frequencies. In the downwind direction as shown in Figure 17(b) the data points fall above the spherical spreading curve and decay in level at a rate which approaches 3 dB per doubling of distance. This is in marked contrast to the data presented earlier for the higher frequencies. The reason for this result is not known but it suggests either the presence of a surface wave phenomenon previously identified in theoretical studies (Ref. 2), or a near-ground level chaneling effect due to refraction.

CONCLUSIONS

An experimental and analytical study of sound propagation for distances up to 1050 m from a large wind turbine noise source, for mean wind speeds in the range 9.4-13.0 m/s has led to the following conclusions:

1. At frequencies above 63 Hz in the downwind and crosswind directions the sound pressure levels decay with distance according to predictions based on atmospheric absorption and spherical spreading.

2. In the upwind direction at frequencies above 63 Hz there is excess attenuation resulting from the existence of an acoustic shadow zone.

-11-

3. The assumption of a distributed noise source (rotor dis'` rather than an acoustic point source, gives better estimates of far field noise in the upwind direction where the formation of acoustic shadows is significant.

4. For very low frequencies (8-16 Hz) there is no observed excess attenuation in the upwind acoustic shadow zone at distances up to 1050 m. In the downwind direction the decay of sound pressure level with distance was less than that predicted by spherical spreading.

WTS-4 HORIZONTAL AXIS WIND TURBINE GENERATOR

Location of wind turbine generator test site

WYOMING
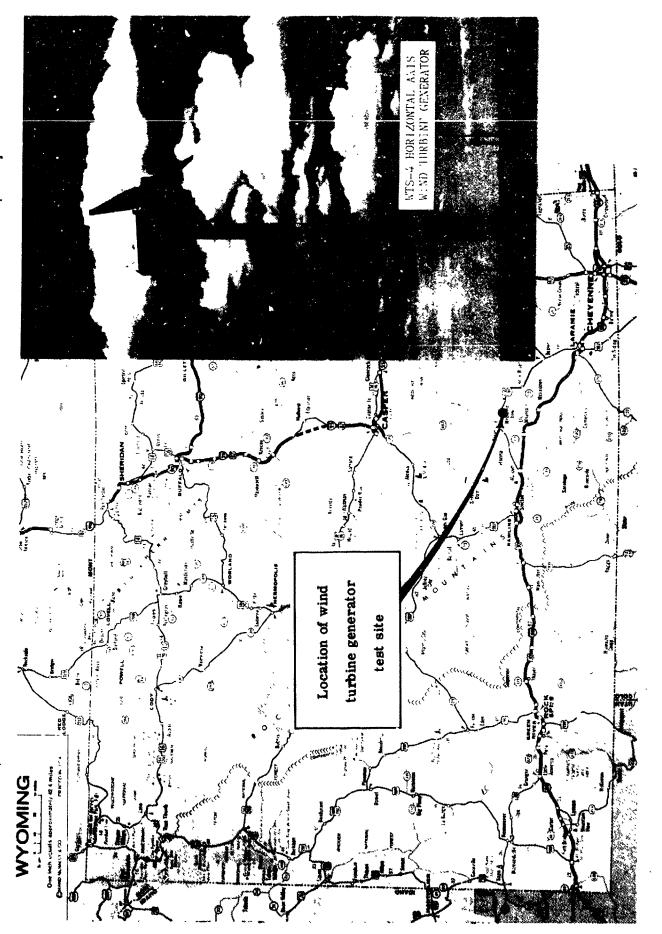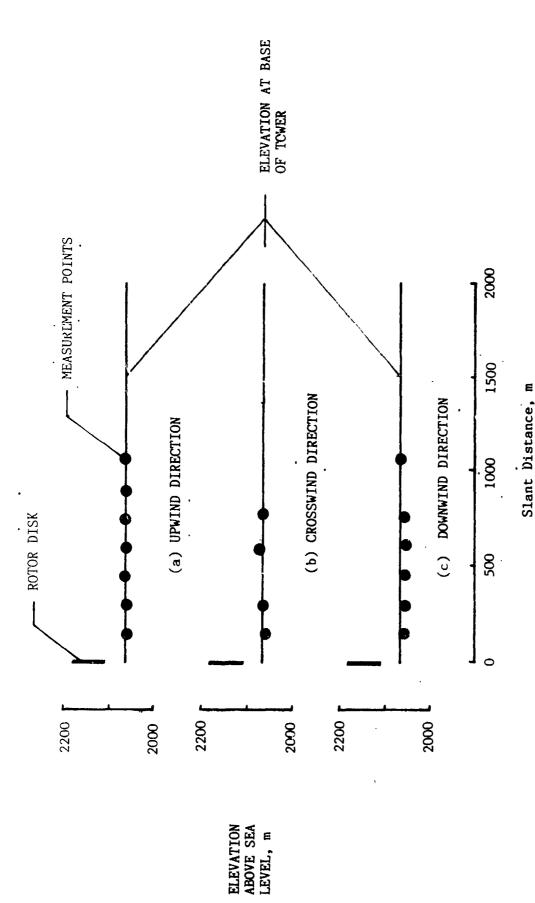
FIGURE 1.   DEPARTMENT OF THE INTERIOR (DOI) BUREAU OF RECLAMATION
WTS-4 WIND TURBINE TEST SITE.

FIGURE 2. ELEVATIONS OF ACOUSTIC MEASUREMENT POINTS
AT VARIOUS DISTANCES UPWIND, CROSSWIND AND
DOWNWIND FROM THE WTS-4 MACHINE.

(a) WIND SPEED

(b) WIND DIRECTION

TIME

5 m/s

20 Deg.

120 Sec.
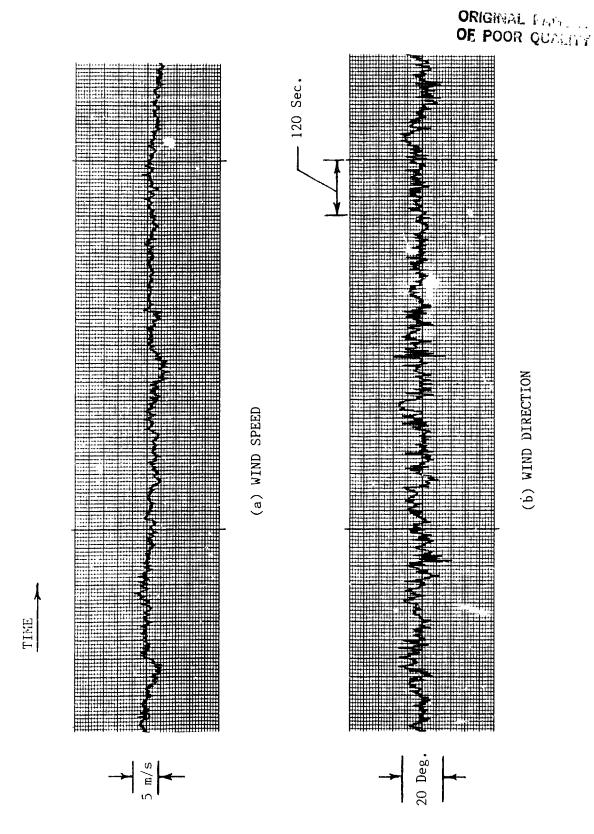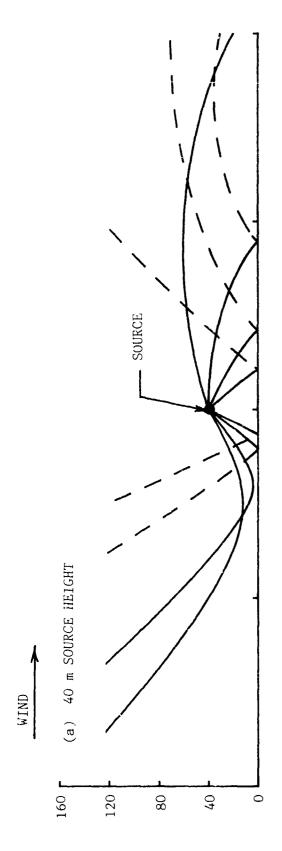
FIGURE 3.   REPRESENTATIVE TIME HISTORIES OF WIND SPEED
AND DIRECTION.

WIND →

(a) 40 m SOURCE HEIGHT

SOURCE

(b) 120 m SOURCE HEIGHT

SOURCE

HEIGHT ABOVE
GROUND, m

160   120   80   40   0

160   120   80   40   0

2000   1000   0   1000   2000

Distance, m
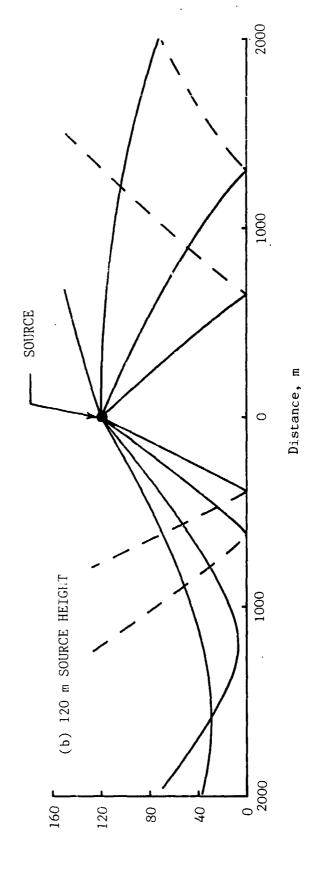
FIGURE 4.   RAY PATH DIAGRAMS UPWIND AND DOWNWIND FROM A
POINT SOURCE AT TWO DIFFERENT HEIGHTS.

-16-

(a) DOWNWIND

(b) UPWIND

DISTRIBUTED SOURCE

GROUND SURFACE

SHADOW

DISTANCE

DISTANCE

V
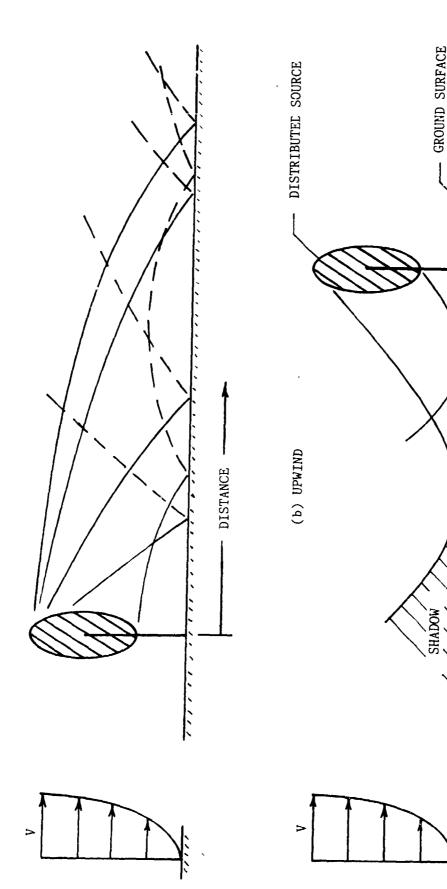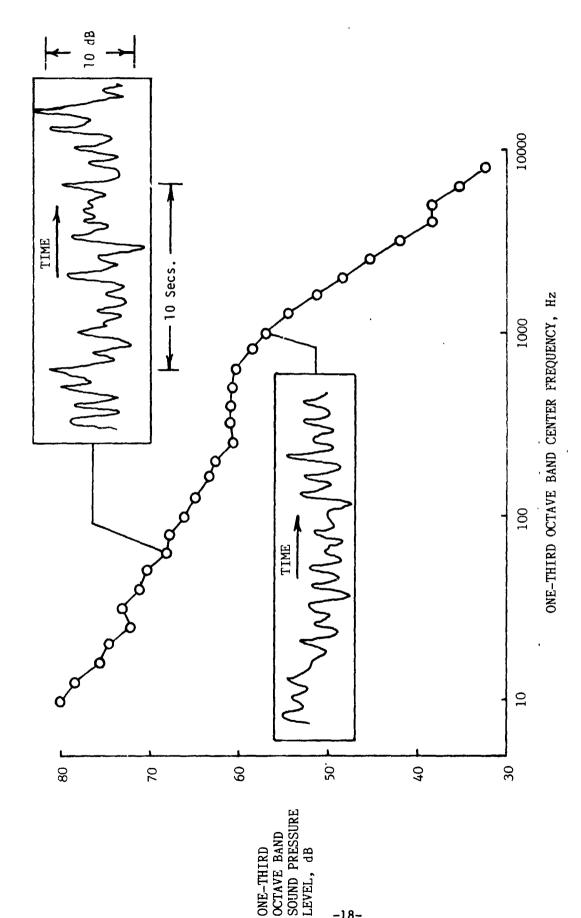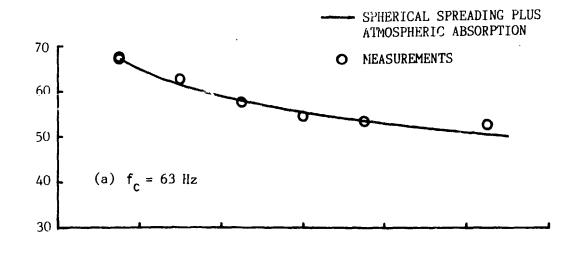
FIGURE 5.   RAY PATH DIAGRAMS DOWNWIND AND UPWIND OF A
DISTRIBUTED SOURCE, INDICATING THE REFRACTION
EFFECTS OF A MEAN WIND GRADIENT.
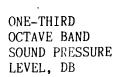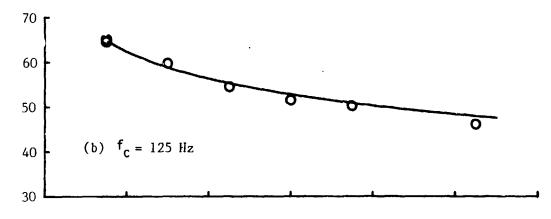
FIGURE 6. ONE-THIRD OCTAVE BAND SPECTRUM OF THE WIND TURBINE NOISE MEASURED AT 150 m AT GROUND LEVEL. INSETS ARE SOUND PRESSURE LEVEL TIME HISTORIES (AVERAGING TIME = 0.2 SECS.) FOR TWO DIFFERENT FREQUENCY BANDS.

ONE-THIRD OCTAVE BAND SOUND PRESSURE LEVEL, dB

ONE-THIRD OCTAVE BAND CENTER FREQUENCY, Hz
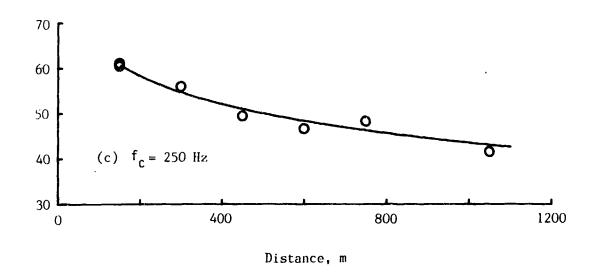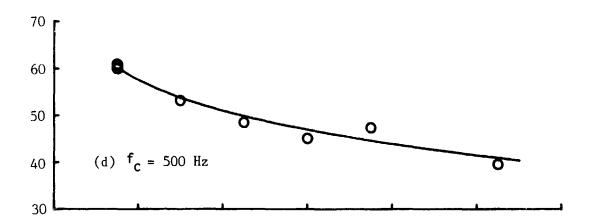
FIGURE 7. SOUND PRESSURE LEVELS AS A FUNCTION
OF DISTANCE DOWNWIND FROM THE MACHINE
FOR VARIOUS FREQUENCY BANDS.

ONE-THIRD
OCTAVE BAND
SOUND PRESSURE
LEVEL, dB

(d) f_c = 500 Hz

(e) f_c = 1000 Hz

Distance, m

FIGURE 7. (Concl.)

-20-
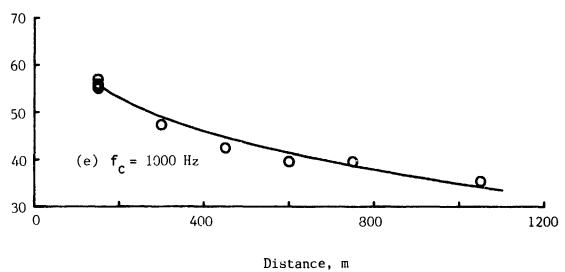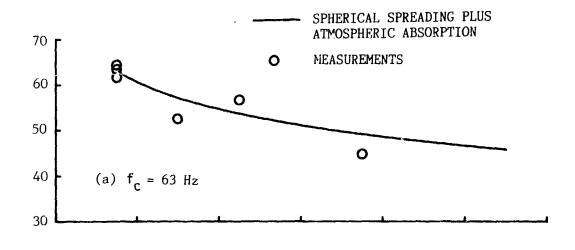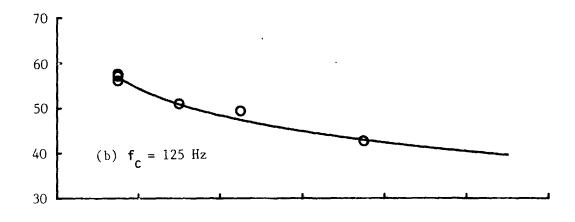
ONE-THIRD
OCTAVE BAND
SOUND PRESSURE
LEVEL, dB

FIGURE 8. SOUND PRESSURE LEVELS AS A FUNCTION OF
DISTANCE CROSSWIND FROM THE MACHINE
FOR VARIOUS ONE-THIRD OCTAVE FREQUENCY
BANDS.
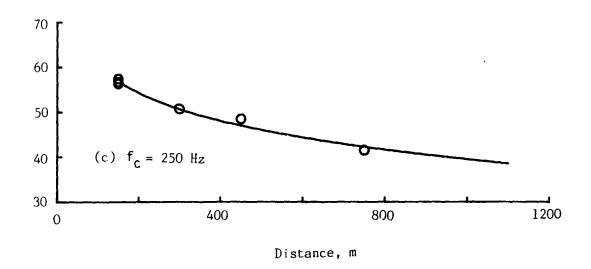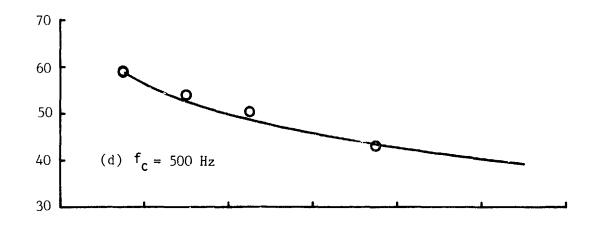
ONE-THIRD
OCTAVE BAND
SOUND PRESSURE
LEVEL, dB

(d) f_c = 500 Hz

(3) f_c = 1000 Hz

Distance, m
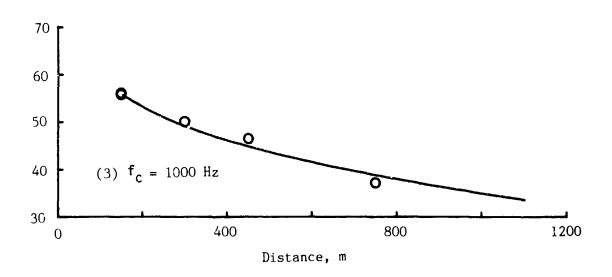
FIGURE 8. (Concl.)
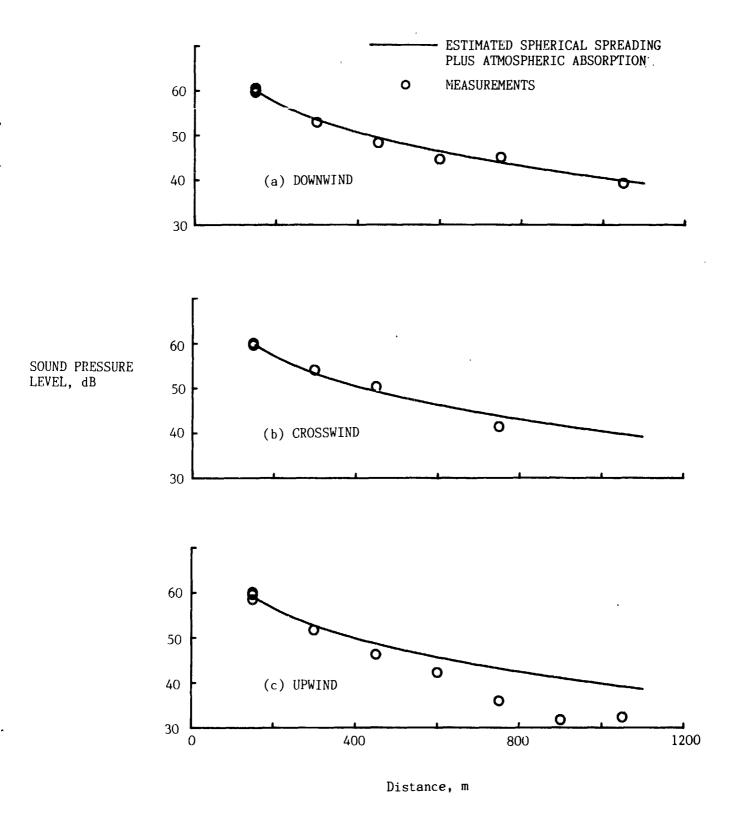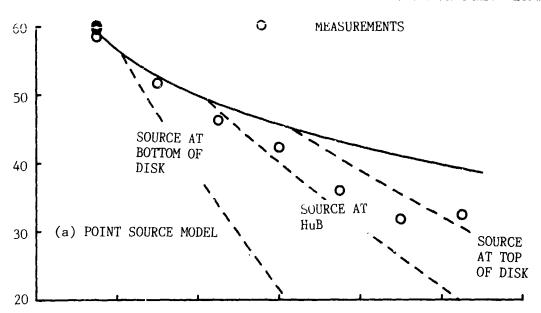
FIGURE 9. SOUND PRESSURE LEVELS IN THE 630 Hz THIRD OCTAVE BAND AS A FUNCTION OF DISTANCE FROM THE MACHINE IN THREE DIFFERENT DIRECTIONS.

-23-

FIGURE 10. COMPARISONS OF MEASURED AND CALCULATED 630 Hz
ONE-THIRD OCTAVE BAND SOUND PRESSURE LEVELS
AS A FUNCTION OF DISTANCE FROM THE MACHINE.
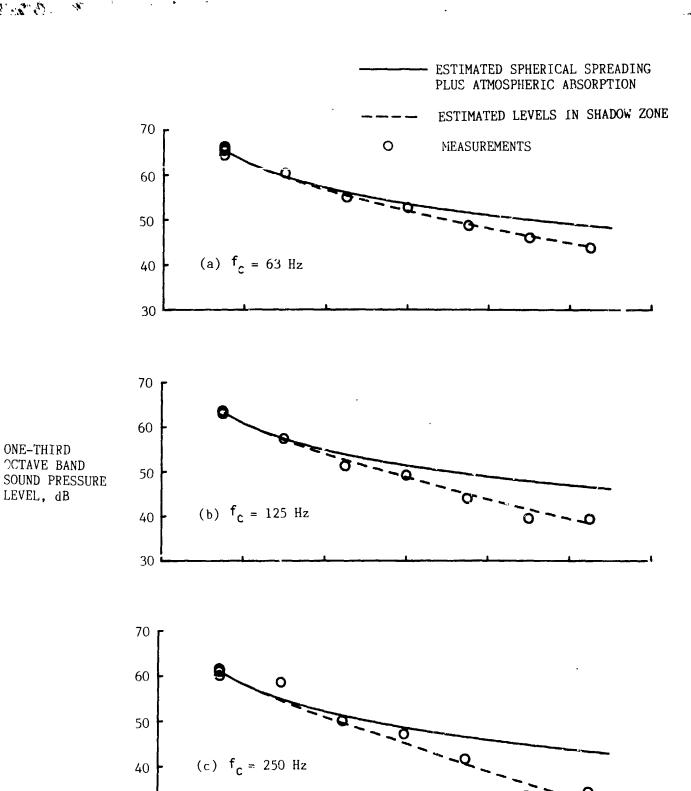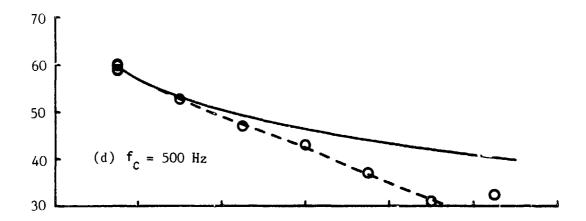
FIGURE 11.   SOUND PRESSURE LEVELS AS A FUNCTION
             OF DISTANCE UPWIND FROM THE MACHINE
             FOR VARIOUS ONE-THIRD OCTAVE FREQUENCY
             BANDS.

ONE-THIRD
OCTAVE BAND
SOUND PRESSURE
LEVEL, dB

(d) f_C = 500 Hz

(e) f_C = 1000 Hz

Distance, m

FIGURE 11. (Concl.)

-26-

STATISTICAL MEASURES

L_1

L_{10}

L_{50}

L_{90}

L_{99}

TIME

10 Secs.

5 Revs.

SOUND PRESSURE
LEVEL, dB

66

62

58

54
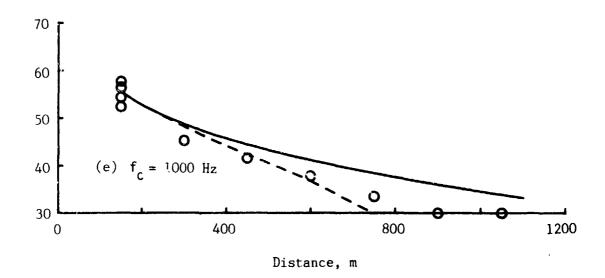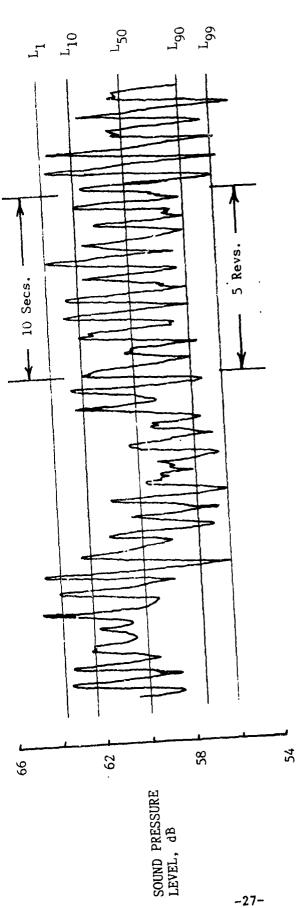
FIGURE 12.   TIME HISTORY OF THE 630 Hz ONE-THIRD OCTAVE
BAND SOUND PRESSURE LEVEL (AVERAGING TIME =
0.2 secs.), WITH DEFINITIONS OF VARIOUS
STATISTICAL MEASURES OF SOUND PRESSURE
LEVEL DISTRIBUTION.

-27-
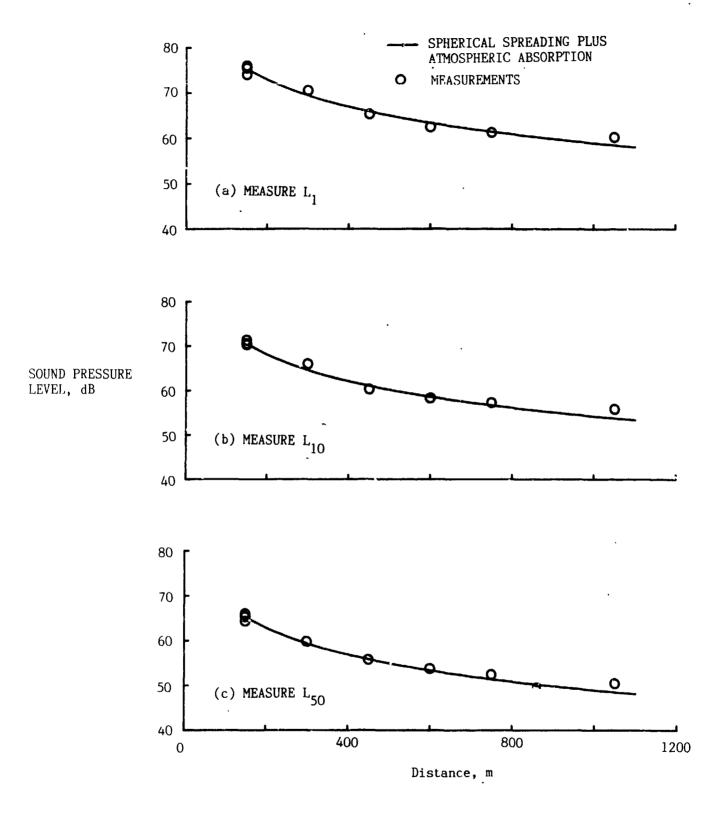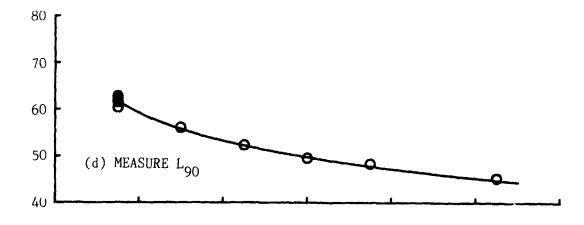
FIGURE 13.   SOUND PRESSURE LEVELS FOR VARIOUS STATISTICAL
             MEASURES OF THE NOISE IN THE 63 Hz ONE-THIRD
   OCTAVE BAND DOWNWIND OF THE MACHINE.

SOUND PRESSURE
LEVEL, dB

(d) MEASURE L_{90}

(e) MEASURE L_{99}

Distance, m

FIGURE 13. (Concl.)

SPHERICAL SPREADING PLUS
ATMOSPHERIC ABSORPTION

O   MEASUREMENTS

(a) MEASURE L_1

SOUND PRESSURE
LEVEL, dB

(b) MEASURE L_{10}

(c) MEASURE L_{50}

Distance, m
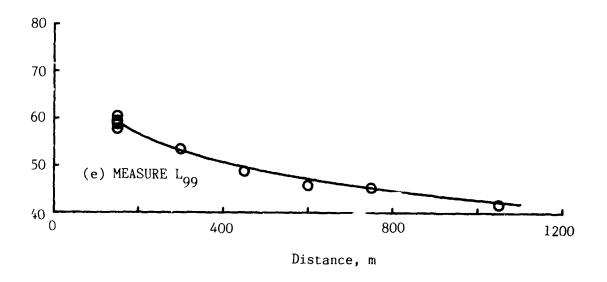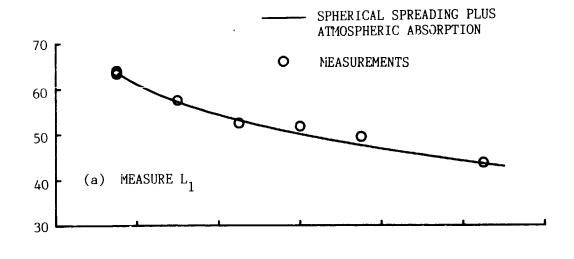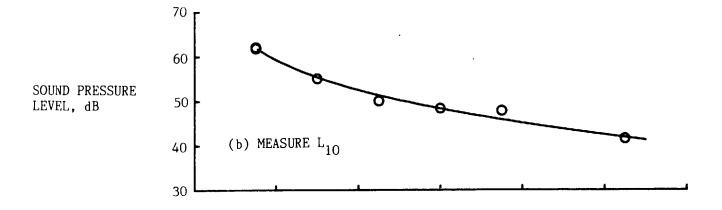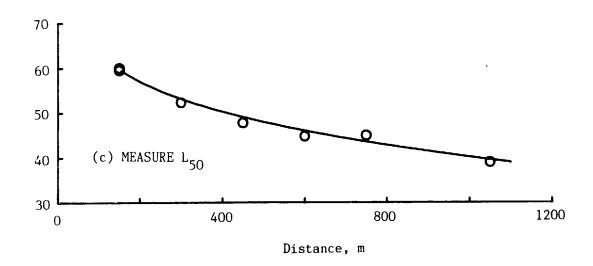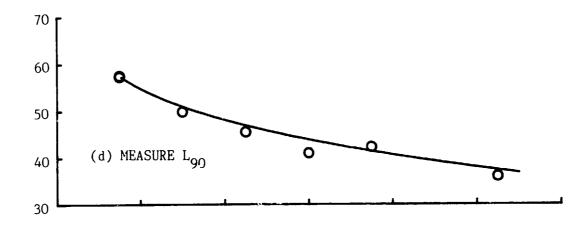
FIGURE 14.   SOUND PRESSURE LEVELS FOR VARIOUS STATISTICAL
MEASURES OF THE NOISE IN THE 630 Hz ONE-THIRD
OCTAVE BAND DOWNWIND OF THE MACHINE.

SOUND PRESSURE
LEVEL, dB

(d) MEASURE L_{90}

(e) MEASURE L_{99}

Distance, m

FIGURE 14. (Concl.)
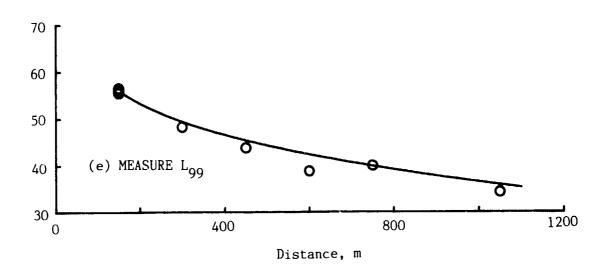
FIGURE 15. SOUND PRESSURE LEVELS FOR VARIOUS STATISTICAL
MEASURES OF THE NOISE IN THE 63 Hz ONE-THIRD
OCTAVE BAND UPWIND OF THE MACHINE.

-32-

SOUND PRESSURE
LEVEL, dB

(d) MEASURE L_{90}

(e) MEASURE L_{99}

Distance, m

FIGURE 15. (Concl.)

-33-
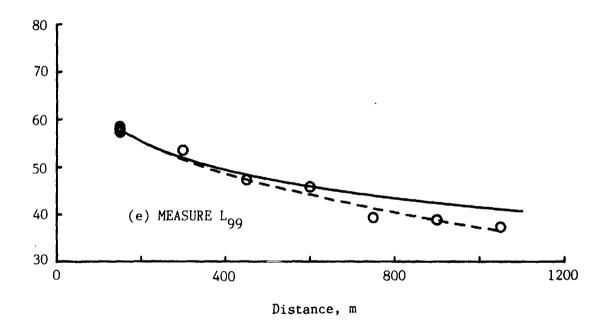
FIGURE 16. SOUND PRESSURE LEVELS FOR VARIOUS STATISTICAL
MEASURES OF THE NOISE IN THE 630 Hz ONE-THIRD
OCTAVE BAND UPWIND OF THE MACHINE.

SOUND PRESSURE
LEVEL, dB

(d) MEASURE L_{90}

(e) MEASURE L_{99}

Distance, m

FIGURE 16. (Concl.)
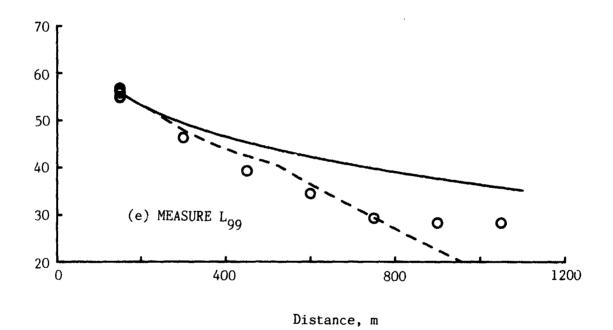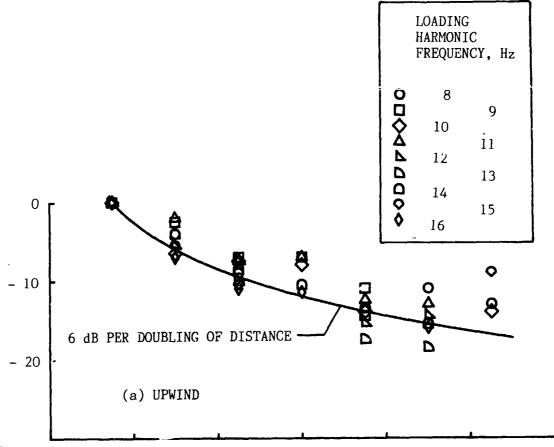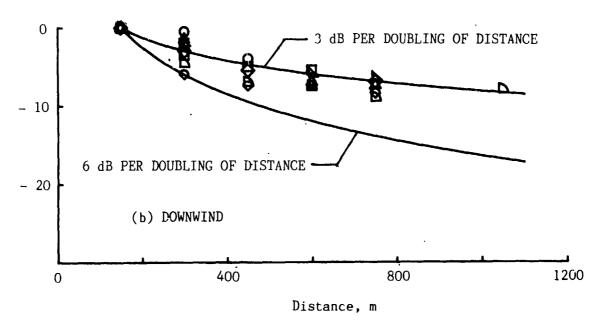
FIGURE 17. MEASURED SOUND PRESSURE LEVELS OF SEVERAL VERY LOW FREQUENCY LOADING HARMONICS AS A FUNCTION OF DISTANCE BOTH UPWIND AND DOWNWIND OF THE MACHINE.

APPENDIX

PREDICTION OF EXCESS ATTENUATION WITHIN THE UPWIND SHADOW ZONE

Following is a description of the methods and assumptions used in the computation of the prediction (dashed) curves presented in Figures 10, 11, 15 and 16. The location of the shadow zone and the excess attenuation which occurs within it are computed for both an acoustic point source and a distributed source which represents a wind turbine rotor disk.

LOCATION OF SHADOW ZONE

The motion of an infinitesimal section of an acoustic wave front is in a direction which is the resultant of the vector of its wave velocity (the speed of sound), which is normal to the wave front, and the vector of the wind velocity. The path traced out by such a section of the wave front is the ray path.

As indicated in the ray path diagrams of Figures 4 and 5, refraction due to a wind gradient results in the formation of a shadow zone upwind of an acoustic source. The distance from the source to the edge of this shadow zone is dependent upon the wind velocity gradient and the elevation of the source above the ground surface. Acoustic ray paths for propagation directly upwind have been calculated for a range of wind velocities and source heights. The wind velocity gradient was assumed to be of the form:

$$V_z = V_f \, K \, \log_e \left(1 + \frac{z}{z_o} \right)$$

where V_z is the wind velocity at height z, K is a constant (2.5), V_f is a friction velocity, and Z_o is a roughness length. Both V_f and Z_o are functions of the characteristics of the terrain over which the wind is blowing. For the present example a value of 0.1 m was chosen for Z_o.

The ray which just grazes the ground surface defines the edge of the wind shadow zone for a ground level receiver (Figure 4). For the range of wind velocities for which acoustic data are available (10-15 m/s at hub height), the horizontal distance from the source to the edge of the shadow zone was calculated to be approximately (5.25 x h), where h is the source height, assumed to be in the range 40-120 m (the elevation of the rotor disk).

EXCESS ATTENUATION

Attenuation in excess of that predicted by spherical spreading and atmospheric absorption is found in the shadow zone. This excess attenuation is frequency dependent, the lowest frequencies being attenuated the least (Refs. 1 and 2). For the present calculations an empirical scheme based on information in Refs. 1 and 2 was employed and is illustrated in Figure A1. The excess attenuation, D, is frequency dependent and is assumed to take place over a distance equal to twice that from the source to the edge of the shadow zone (distance x). Thus, the predicted decay of sound pressure level with distance was based on atmospheric absorption (Ref. 1) and spherical spreading from the source to the edge of the shadow zone. Beyond this distance, extra attenuation given by Figure A1 was added.

DISTRIBUTED ACOUSTIC SOURCE

A wind turbine is considered a distributed source since aerodynamic noise is generated from all portions of the rotor disk described by the rotating blades as they interact with the aerodynamic flow. The distribution of noise on the rotor blade is determined by several factors including blade area, blade chord, inflow turbulence, trailing edge thickness and blade section speed (Ref. 3). The factor having the greatest influence on the noise generation is blade section speed. For the present calculations the noise distribution on
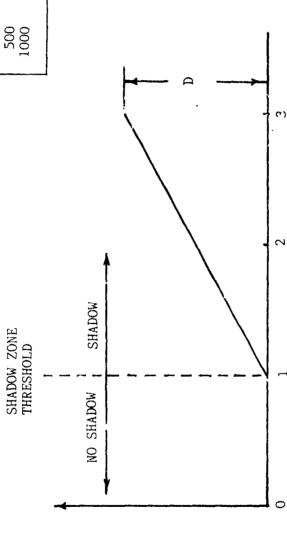
the rotor blade was simply assumed to be proportional to the blade section
speed raised to the power 5.

An array of sources was assumed and their contributions were summed both
radially and circumferentially. Twenty stations equally spaced along the blade
diameter were chosen. Each station was treated as a point source and the decay
of sound pressure level with distance was computed using the procedure
described in the previous section of this Appendix. Summing the contributions
from each of the point sources thus yielded the decay of sound pressure level
with distance for a given rotor position. This procedure was repeated for
rotor position angles from $0°$ to $180°$, at $1°$ intervals, in order to integrate
over one complete revolution of the turbine. Thus the decay of sound pressure
level with distance, integrated over the entire rotor disk, was calculated.
The statistical measures (L_1, L_{10}, L_{50}, etc.) were calculated from a time history
derived from the integrated sound pressure levels calculated for each rotor
position from $0°$ to $180°$.

The decay of sound pressure level with distance for a distributed source
is schematically illustrated in Figure A2. At short distances from the wind
turbine, sound is received from the entire rotor disk (distributed source) and
there is no excess attenuation. As the distance is increased a shadow zone
formed by the bottom of the disk is encountered. This results in a very small
excess attenuation, because only a small portion of the disk is shadowed. This
process continues until the entire disk is shadowed. Excess attenuation
increases with distance beyond this point until a limiting value of D (Figure
A1) is achieved.

FREQ, Hz	D, dB
63	6
125	12
250	18
500	24
1000	30

SHADOW ZONE
THRESHOLD

NO SHADOW   SHADOW

EXCESS
ATTENUATION,
dB
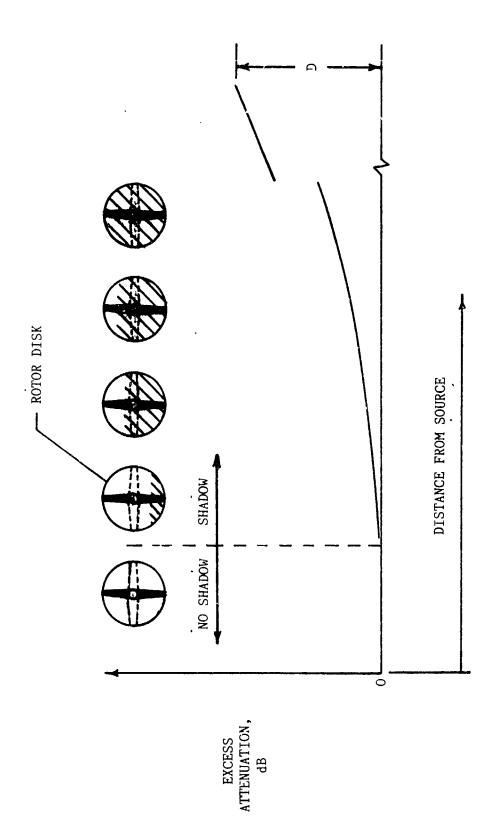
DISTANCE FROM SOURCE, x

FIGURE A1.   EXCESS SHADOW ZONE ATTENUATION AS A FUNCTION
OF DISTANCE FROM A POINT SOURCE.

FIGURE A2. EXCESS SHADOW ZONE ATTENUATION AS A FUNCTION OF DISTANCE FROM A DISTRIBUTED SOURCE.

REFERENCES

1. Anonymous: American Standard Method for the Calculation of the Absorption of Sound by the Atmosphere. ANSI 21.26-1978.

2. Piercy, J. E., Embleton, T. F. W., and Sutherland, L. C.: Review of Noise Propagation in the Atmosphere. JASA Vol. 61, No. 6, June 1977.

3. Weiner, Francis M. and Keast, David N.: Experimental Study of the Propagation of Sound Over Ground. JASA Vol. 31, No. 6, June 1959.

4. Anonymous: Method for Calculating the Attenuation of Aircraft Ground to Ground Noise Propagation During Takeoff and Landing. SAE Aerospace Information Report A^{TD} 923, August 1966.

5. Shepherd, Kevin P. and Hubbard, Harvey H.: Measurements and Observations of Noise from a 4.2 Megawatt (WTS-4) Wind Turbine Generator. NASA CR-166124, May 1983.

6. Grosveld, F. W., Shepherd, K. P., and Hubbard, H. H.: Measurement and Prediction of Broadband Noise from Large Horizontal Axis Wind Turbine Generators. Presented at NASA/DOE Workshop on Horizontal Axis Wind Turbine Technology, Cleveland, Ohio, May 8-10, 1984.

7. Grosveld, F. W.: Prediction of Broadband Noise from Large Horizontal Axis Wind Turbine Generators. Preprint No. AIAA-84-2357, October 1984.